Chemistry of Urban Grime: Inorganic Ion Composition of Grime vs Particles in Leipzig, Germany

ARTICLE *in* ENVIRONMENTAL SCIENCE & TECHNOLOGY · SEPTEMBER 2015

Impact Factor: 5.33 · DOI: 10.1021/acs.est.5b03054

6 AUTHORS, INCLUDING:

Konrad Mueller

Leibniz Institute for Tropospheric Research

181 PUBLICATIONS **1,777** CITATIONS

SEE PROFILE

Hartmut Herrmann

Leibniz Institute for Tropospheric Research

751 PUBLICATIONS **7,038** CITATIONS

SEE PROFILE

D.J. James Donaldson

University of Toronto

191 PUBLICATIONS **4,592** CITATIONS

SEE PROFILE

Environmental Science & Technology

Article

pubs.acs.org/est

Chemistry of Urban Grime: Inorganic Ion Composition of Grime vs Particles in Leipzig, Germany

Alyson M. Baergen,[†] Sarah A. Styler,[‡,§] Dominik van Pinxteren,[‡] Konrad Müller,[‡] Hartmut Herrmann,[‡] and D. James Donaldson*[,†,∥]

[†]Department of Chemistry, University of Toronto, 80 St. George Street, Toronto, Ontario, Canada M5S 3H6

[‡]Atmospheric Chemistry Department (ACD), Leibniz-Institut für Troposphärenforschung (TROPOS), Permoserstrasse 15, 04318 Leipzig, Saxony, Germany

[∥]Department of Physical and Environmental Sciences, University of Toronto Scarborough, 1265 Military Trail, Toronto, Ontario M1C 1A4, Canada

Supporting Information

ABSTRACT: Deposition of atmospheric constituents - either gas phase or particulate - onto urban impervious surfaces gives rise to a thin "urban grime" film. The area exposed by these impervious surfaces in a typical urban environment is comparable to, or greater than, that of particles present in the urban boundary layer; however, it is largely overlooked as a site for heterogeneous reactions. Here we present the results of a field campaign to determine and compare the chemical composition of urban grime and of particles collected simultaneously during the autumn of 2014 at an urban site in central Leipzig, Germany. We see dramatically reduced ammonium and nitrate levels in the film as compared to particles, suggesting a significant loss of ammonium nitrate, thus enhancing the mobility of these species in the environment. Nitrate levels are 10% lower for films exposed to sunlight compared to those that were shielded from direct sun, indicating a possible mechanism for recycling nitrate anion to reactive nitrogen species. Finally, chloride levels in the film suggest that urban grime could represent an unrecognized source of continental chloride available for $ClNO_2$ production even in times of low particulate chloride. Such source and recycling processes could prove to be important to local and regional air quality.

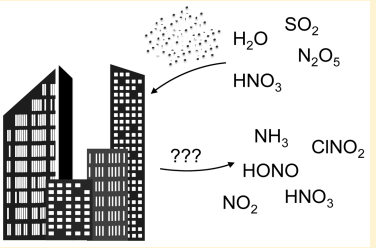

INTRODUCTION

Heterogeneous and multiphase reactions are important in the troposphere, promoting reactions that are not favorable in the gas phase.[1] N_2O_5 and NO_2 hydrolysis,[2,3] $ClNO_2$ formation,[4,5] heterogeneous SO_2 oxidation,[6] interactions of trace gases with mineral dust components,[7,8] and surface photochemistry[9] are all examples of such important atmospheric-surface interactions. The studies of these reactions are usually limited to particle and sea surfaces; however, in an urban setting, there are many impervious surfaces, such as buildings, roadways, and windows, providing another type of surface that is often overlooked despite having a combined surface area estimated to be similar to that of atmospheric particles.[10,11] When impervious surfaces are exposed to the atmosphere surface films form over time.[12−26] Sometimes referred to as urban grime, the films are a complex mixture of species formed via the deposition and subsequent processing of atmospheric species.[27]

Models have been developed which try to characterize the growth of urban grime and give insight into the growth mechanism. Many of these are empirical models, fitting observed changes in total film mass, in a particular constituent's mass, or in optical properties to descriptive equations as a function of time.[17,20,28] These models highlight the complexity of the growth mechanisms and the variability of film formation depending on location. More recently the models have been further parametrized to include atmospheric measurements, giving more insight into the growth mechanism. They show that PM_{10} is the dominant driver for film formation but also that the inclusion of SO_2 and NO_2 into the models allows for a better fit to the observed growth characteristics.[29,30] Semi-volatile compounds have also been observed to approach an equilibrium between the film and surrounding atmosphere,[25] implying dynamic partitioning behavior, and polymers have been detected that are suggested to form through reactions within the film.[16] This highlights that grime is not merely a collection of deposited particles but rather is a dynamic system, which is influenced by the continued exposure to the atmosphere.

While such models are helpful in understanding film formation, they say little about the potential environmental impact of urban grime. Diamond and co-workers have begun to address this issue by developing regional models which include film dynamics, showing that the films enhance the mobility of organic constituents in the environment through partitioning and water runoff.[10,11,31,32] At this point, however, there is

Received: June 29, 2015
Revised: September 23, 2015
Accepted: September 30, 2015

DOI: 10.1021/acs.est.5b03054
Environ. Sci. Technol. XXXX, XXX, XXX−XXX

limited work on inorganic species and understanding the films as a reactive environment. Reactive studies have been limited to the use of organic proxy films, such as PAH films, a mixture of potassium nitrate and pyrene, or octanol spread on a film of silicone vacuum grease.[33−41] The exception is our recent laboratory report on nitrate photochemistry within real grime, which demonstrated that the grime-associated nitrate is photolabile.[42]

In the current study, we measured the composition of one of the major sources of these films, PM_{10} (particles smaller than 10 μm in diameter), simultaneously with that of grime samples collected at the same location. The inorganic composition will be the focus of this paper, while the organic composition will be reported separately. There has been only a single study published to date in which particle composition was measured simultaneously to that of grime, with the particles being collected over 3 months using an air filtration unit.[22] Further investigation is clearly warranted, using a more standardized particle sampling method and with samples taken at a higher time frequency to more fully track the formation of the grime in the context of changing particle concentrations. The goal of the present study is to utilize the comparison of particle and grime compositions during initial grime formation to begin to identify grime-mediated processes that could impact environmental cycling of some key chemical species. Here we also report the first measurement of urban grime photochemistry derived from field measurements using real sunlight.

EXPERIMENTAL SECTION

Sampling of urban grime and atmospheric particles was carried out in Leipzig, Germany between September 16 and October 25, 2014 at the "Leipzig-Mitte" (51.33°N, 12.38°E) site described previously.[43] Briefly, this is a roadside site at the corner of a major intersection opposite the main train station in the middle of Leipzig. Figure S1a of the Supporting Information (SI) shows a photograph of the sampling site. Local meteorological, NO_x and SO_2 measurements were collected over the duration of the campaign from the same location by the Saxon State Agency for Environment, Agriculture and Geology and are presented in Figure S2.

Film Sampling. Film samples were collected by exposing 3 mm diameter soda-lime glass beads (Sigma-Aldrich) to the atmosphere. These beads, similar to those used by Wu et al.,[24,25] were chosen to provide a high surface area surrogate for common window glass. A possible impact of using bead surrogates is that the geometry of the beads, with both horizontal and vertical surfaces, may favor the collection of larger particles in comparison to vertical window surfaces.[44] Beads were prepared by soaking in a base bath for 1 h followed by rinsing the beads ten times with tap water, soaking overnight in deionized water, and further rinsing eight times in deionized water. They were then baked in a 100 °C oven overnight to remove residual water.

Beads were divided into 80.0 g samples, and each sample was placed into one of the 48 compartments within the sampler, forming a single layer of beads, as illustrated in Figure S1b. The sampler was built out of stainless steel with stainless steel mesh tray bottoms and open sides to allow gas flow. It was covered by a *Plexiglas GS, UV transmitting clear 2458* window, shielding the sampler from precipitation while allowing light through to the samples. The beads were further protected from precipitation with metal slats around the outside of each layer, which could be removed to access the beads. As shown in Figure S1, there were three trays of beads. Only the top two were used for this study. Below the first level of beads there was a sheet of stainless steel shielding the bottom two levels of beads from direct sunlight. In this way, light-exposed and light-shielded samples were collected in parallel, and thus photochemistry occurring on the film could be probed.

The grid boxes of each tray were numbered from one to 16. Once every 3 days, a grid box number was selected using a random number generator. At 11:00 local time (GMT+2) all of the beads for each of the "light" and "dark" samples corresponding to the chosen number were collected into amber vials for transport. Samples were kept refrigerated until analysis. Field blanks were measured by placing three 80.0 g bead samples onto the sampler and then collecting immediately. Laboratory blanks were also analyzed in which three clean 80.0 g bead samples were analyzed without being transported to the field site.

For analysis, 4.0 g of beads were transferred to a Nalgene bottle and extracted into 3.00 mL of deionized water by shaking the bead/water mixture for 5 min, while the remaining 76.0 g of beads were used for analysis of the organic components of the film. The aqueous extract was removed and analyzed for ions as described below. The extraction efficiency was examined by performing serial extractions in which a previously analyzed sample was extracted for a second time. For all ions, less than 9% remained in the second extraction. While attempts were made to allow equal airflow to all compartments in the sampler, there is some variability depending on location in the sampler. To examine this variability between samples, samples were taken from three different compartments on October 7, 2014, indicating less than 35% deviation from the mean value. This is shown in Figure S3.

Particle Sampling. PM_{10} (particles below 10 μm in diameter) were sampled through an inlet with a 10 μm cutoff for 72 h (11:00−11:00 local time) with a "Partisol 2000" low volume sampler at a sampling rate of 1.0 m^3/h. Particles were collected onto 45 mm diameter quartz filters which were preconditioned by heating at 105 °C for 24 h. Sections of the filter (1 cm^2) were removed for organic carbon/elemental carbon analysis, while two 6 mm diameter circles were removed for GC-MS analysis of PAHs and alkanes. The remaining filter area (1434 mm^2) was extracted into 1.50 mL of deionized water through 10 min of sonication, 10 min of shaking, and a further 10 min of sonication. Beginning on October 20, 2015, the composition of size-resolved particles was also determined by collecting samples using a five-stage (stage 1:0.05−0.14 μm, stage 2:0.14−0.42 μm, stage 3:0.42−1.2 μm, stage 4:1.2−3.5 μm, stage 5:3.5−10 μm, aerodynamical particle diameter) stainless steel low pressure Berner impactor (Hauke, Austria) with a flow rate of 4.5 m^3/h.[45] The particles were collected onto aluminum foil for 24 h, and a fraction of this foil was extracted into 2.00 mL of deionized water using the technique described above for filters. Foils had a calcium contamination contributing up to 89% of the measured calcium mass. Reported values were corrected by subtracting the average of the blank values from the sample measurements, with the exception of two samples from stage 1 which were within error of the blank values and are reported as 0 $\mu g/m^3$.

Because 3-day filter collection times were used, we expect the occurrence of sampling artifacts such as volatilization of high vapor pressure compounds like ammonium nitrate and small organics.[22] Similar processes are expected for the aging of film samples, thus biasing the measured particle compositions

DOI: 10.1021/acs.est.5b03054
Environ. Sci. Technol. XXXX, XXX, XXX−XXX

toward that of the grime film. Therefore, the film and particle composition may appear more similar than they are in reality. However, we note that the particle filter was within a temperature controlled environment, with the temperature maintained at 20.7 ± 0.4 °C. Therefore, the collected filter samples did not undergo the same temperature cycles as the film (as shown in Figure S2a).

Ion Analysis. All aqueous extracts were filtered using a 0.45 μm Acrodisc syringe filter to remove insoluble materials. The resulting solutions were analyzed using ion chromatography to detect the main water-soluble ions (Cl^-, SO_4^{2-}, NO_3^-, $C_2O_4^{2-}$, NH_4^+, Na^+, K^+, Ca^{2+}, Mg^{2+}) using a Thermo ion chromatograph (ICS3000) with AS18/AG18 column/guard column with potassium hydroxide eluent for anion analysis and CS16/CG16 column/guard column with methanesulfonic acid eluent for cation analysis. Conductivity detection was used for all ions with the exception of NO_3^- that was detected using UV at 208 nm.

RESULTS

Particle and grime samples were each collected at the Leipzig-Mitte site during the period between September 16 and October 25, 2014, and the major water-soluble ions in each sample type were analyzed via ion chromatography. Figure 1 displays the observed ion mass fractions, Figure 2 displays the molar ratios of ions normalized to total sulfate, and Figures S3 and S4 present the absolute concentrations determined for the particles and light-exposed grime samples, respectively. The variability among the grime samples is indicated in the scatter plots, which show three separate data points (hollow circles) for the three grime samples collected on October 7. Sulfate was chosen as the normalizing species because it is expected to be stable within the film, having low volatility and photoactivity. We note that there may be additional gas phase sources of sulfate to the film, such as SO_2 deposition and oxidation, akin to particulate sulfate sources,[46] due to the grime's continued exposure to the atmosphere. Chabas and co-workers have also suggested that SO_2 can react with sodium and calcium, either in the film or within the glass substrate, to form salts such as $CaSO_4$ and Na_2SO_4.[18,22] Extra sulfate sources to the film would result in the sulfate-normalized values underestimating additional sources of ions to the film or overestimating the losses of ions from the film. Further study is warranted to establish the relative importance of such sulfate sources in addition to particulate deposition. However, for the subsequent discussion it is assumed that sulfate sources from such heterogeneous reactions are minor in comparison to particulate sulfate sources to the film.

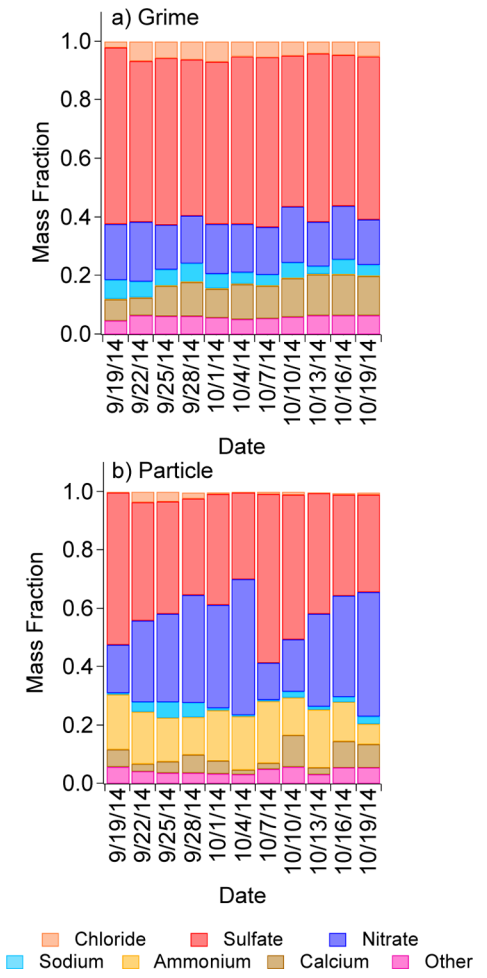

Figure 1. Mass fraction of the major ions Cl^- (orange), SO_4^{2-} (red), NO_3^- (dark blue), Na^+ (light blue), NH_4^+ (yellow), and Ca^{2+} (brown) and the sum of the minor ions $C_2O_4^{2-}$, Mg^{2+}, and K^+ (pink) measured in the a) light-exposed grime and b) particle samples.

In general, we note that the particle ion compositions fall within the range of mass fractions and mass loadings observed at this site in the past.[47] A similar comparison to past film composition measurements is not possible because there are no urban grime composition measurements reported over these time scales, nor are there any reported from this area. However, comparing to the few compositional studies performed in other cities and over much longer time frames, the Leipzig mass fractions are similar to that reported in Paris[22] but generally more sulfate rich and calcium poor than a separate study with film compositions reported from six different European cities.[18]

Depletion of Ammonium and Nitrate in Grime versus Particles. From examination of Figure 1, it is evident that both the film and particle compositions are dominated by the presence of sulfate and nitrate anions. Notably, however, ammonium, which is the dominant cation measured within the particles, is hardly observable within the grime samples. For most samples ammonium was below the detection limit, and thus the values reported herein are the detection limit of the system and represent upper limits to the ammonium present in the film. A contrast between the ammonium presence in particles versus film samples has been reported previously, also indicating that there were low or undetectable levels of ammonium in urban grime films.[18,22] The authors of those previous studies suggested that the lower-than-expected concentration of ammonium is due to the loss of ammonium nitrate. In support of this hypothesis, we observe that nitrate is also significantly lower in the grime than in the particles, most clearly seen by the nitrate-to-sulfate ratio shown in Figure 2c. Ammonium nitrate is semivolatile, and there are many reports of its loss by evaporation from filter samples and particles (e.g., refs 48 and 49). Because the grime film is exposed to the atmosphere for an extended time period, it cycles through different temperature and relative humidity regimes (as displayed in Figure S2). High temperatures and low relative humidities have been shown to favor ammonium nitrate evaporation.[49]

As a further investigation into ammonium nitrate evaporation, the size resolved particle data collected during the final 5

DOI: 10.1021/acs.est.5b03054
Environ. Sci. Technol. XXXX, XXX, XXX−XXX

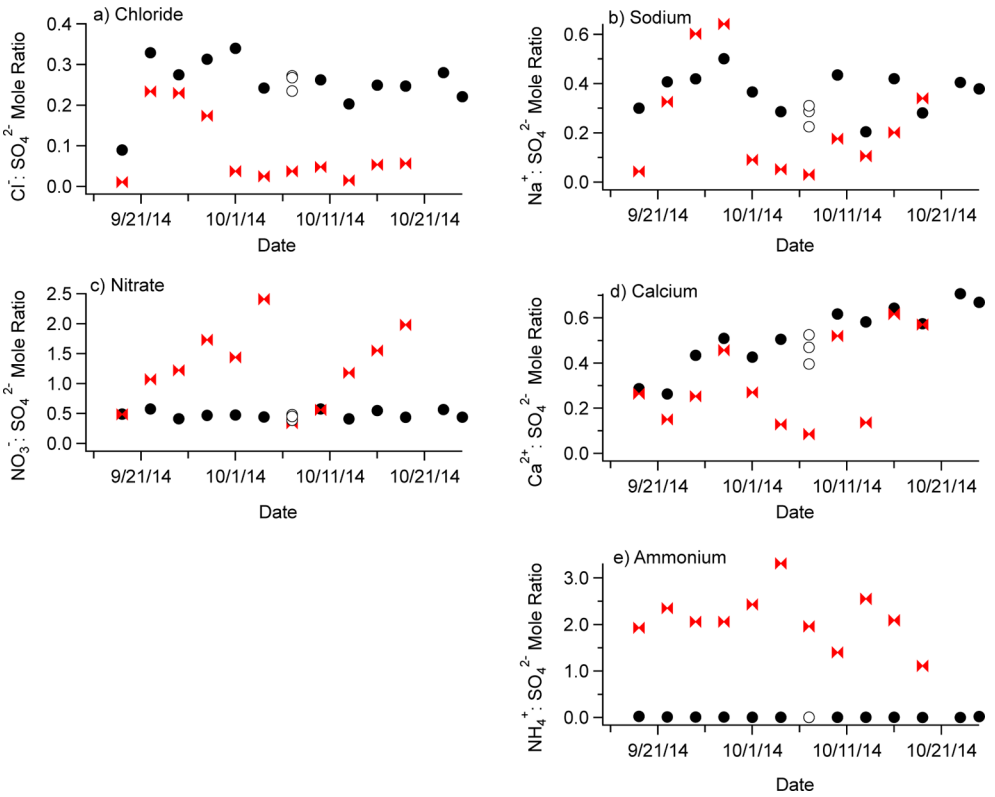

Figure 2. Sulfate normalized mole ratios of a) chloride, b) sodium, c) nitrate, d) calcium, and e) ammonium extracted from film and particle samples. Light-exposed grime values are shown in black circles, while particle values are red bowties. The spread in data from collection and analysis is displayed for the three separate samples collected on October 7, 2014 shown in hollow circles. When ammonium was not detected, values were calculated from the detection limits and are thus upper limits for ammonium in grime.

days of measurements can be examined; this is displayed in Figures S5 and S6 of the SI. The particles rich in ammonium and nitrate are the fine particles in the size bins below 1.3 μm, while the coarse particles, between 1.3 and 10 μm, are ammonium-poor with nitrate likely present as salts such as $Ca(NO_3)_2$.[50] The average nitrate-to-sulfate ratio for the total PM_{10} over the 5 days is 1.4 ± 0.5 (mean ±1 standard deviation), significantly larger than the campaign average of 0.48 ± 0.06 observed for the film. The ratio for particles becomes lower if it is assumed that all of the nitrate associated with deposition of fine-mode particles evaporates as ammonium nitrate, leaving only the coarse mode nitrate. Under this assumption, the average nitrate-to-sulfate mole ratio is reduced to 0.7 ± 0.5, which lies within the uncertainty of the ratio observed in the film. While the possibility of gas phase nitrate sources to the grime such as N_2O_5 or NO_2 hydrolysis or HNO_3 deposition cannot be ruled out, the comparison of these nitrate-to-sulfate ratios suggest the importance of evaporation for much, if not all, of the nitrate that is deposited as ammonium nitrate.

However, if ammonium nitrate loss from deposited particles is the sole mechanism for ammonium depletion (i.e., if the grime ammonium and nitrate amounts are initially the same as those in particles but are then altered via ammonium nitrate evaporation), then we would expect a smaller decrease in the total amount of ammonium than that which is observed in the grime samples. Subtracting the average ammonium-to-sulfate and nitrate-to-sulfate mole ratios in the grime over the course of the campaign from the corresponding average particle ratios, the ammonium-to-sulfate mole ratio decreases by 2.1 ± 0.6 while the nitrate-to-sulfate mole ratio only decreases by 0.8 ± 0.6. Therefore, ammonium nitrate evaporation cannot fully explain the observed loss of ammonium. As shown in the size-resolved particle measurements displayed in Figures S5 and S6, larger particles contain minimal quantities of ammonium, while maintaining moderate amounts of nitrate. If large particles are preferentially deposited and retained on the grime film, or if significant amounts of particles larger than PM_{10} (also expected to show minimal ammonium, see for instance VandenBoer et al.[51]) are deposited onto the grime, this would lower the ammonium fraction measured within the film to a greater extent than for nitrate.

There may also be chemical mechanisms at play that remove the ammonium from the grime film. Favez et al. suggested that ammonium could be lost from grime via either or both of the exchange of ammonium nitrate with NaCl to form $NaNO_3$ and gas phase HCl and NH_3 or the biological conversion of ammonium to nitrate.[18] Another possibility is suggested by the long integration time for collection of the film sample, which could lead to the mixing of the components of the externally mixed coarse and fine particles. This mixing of the particles' components has previously been discussed as a potential artifact for samples collected on filters under high relative humidities,[52] where the presence of water can facilitate ionic mixing. In the present study, the particles were collected in a climate-controlled environment, lowering the possibility of this occurring on the particle filters. However, in the case of grime collected onto glass substrates, we note that glass surfaces are hygroscopic; lab studies also show significant water uptake mediated by the grime film itself.[26,27,42] At the high relative humidities, mostly above 60%, which existed during the

DOI: 10.1021/acs.est.5b03054
Environ. Sci. Technol. XXXX, XXX, XXX−XXX

campaign (shown in Figure S2), there will certainly be water associated with the grime.

Although the ion balance of the particles is quite variable, half of the PM_{10} samples collected measured excess cations; this suggests that the mixture of these ions could be alkaline.[53] Because the larger particle classes contain fewer sulfate and ammonium ions and more of the crustal cations such as sodium and calcium (see Figures S5 and S6), they are more alkaline than the smaller ones. Upon mixing of the components of these more basic particles with those from the smaller acidic ammonium rich particles, there would be an increase in the pH, favoring the formation of ammonia from ammonium. The ammonia could then partition to the gas phase, depending on the local ammonia levels, depleting the film ammonium and giving rise to a smaller proportion of ammonium in the grime than measured in the PM_{10} particles.

Temporal Changes in Grime and Particle Compositions. Figure 2 illustrates that for all of the ions measured here, there is much more variability in particle composition over time than there is for the film. Because the film is continually collecting mass over the course of the campaign, its measured composition results from an integration of particle and gas phase species deposition, evaporative losses, and chemical processing. This long-time averaging has the result that fluctuations in atmospheric composition are smoothed in comparison to the particle samples, which are averaged over a shorter period. Another consequence of this averaging is that the film may maintain a "memory" of periods of time where there is high deposition of a specific chemical species. At the beginning of this campaign, between September 19 and 28, 2015, there was an episode where particles showed high levels of chloride and sodium (see Figure S4). Hysplit back trajectories[54] run for the previous 24 h period suggest that the air mass sampled during that time was mostly transported over the North Sea prior to arriving in Leipzig leading to marine influenced particles, high in sodium and chloride. In these particles, the sodium to chloride mole ratio is above one (2.6 ± 1.1), typical of marine particles undergoing chloride displacement by HNO_3 during transport over continental air.[55] Following September 28, the masses of chloride and sodium in the particles drop due to a shift in the geographic origin of the particles to continental areas.[54] This change in particle composition also results in a drop of both chloride and sodium in the film, as the composition is diluted with particles lower in chloride and sodium, but to a much lesser extent than is evident in the particles.

The change in chloride amount in the grime can be represented by assuming that there is a period, between September 19 and 28, 2014, of fast chloride growth on the film (6.7×10^{-4} μmol/day). The growth rate is calculated from a linear fit of the moles of chloride in the film over time displayed in Figure 3a, where the amount on September 19 is fixed. After September 28, the growth rate is assumed to be 25% of the fast growth rate (1.7×10^{-4} μmol/day) for the remainder of the campaign. This corresponds to the ratio of the average amount of chloride in the particles between September 28 and October 25 to the average chloride content in the particles between September 19 and 28 (Figure S4). By normalizing the resulting growth curves of chloride to experimental sulfate values, these results can be compared to experimental values as shown in Figure 3b. Although there is significant scatter, the calculated chloride values demonstrate that a one-week period of elevated chloride mass in the particles can result in a high chloride

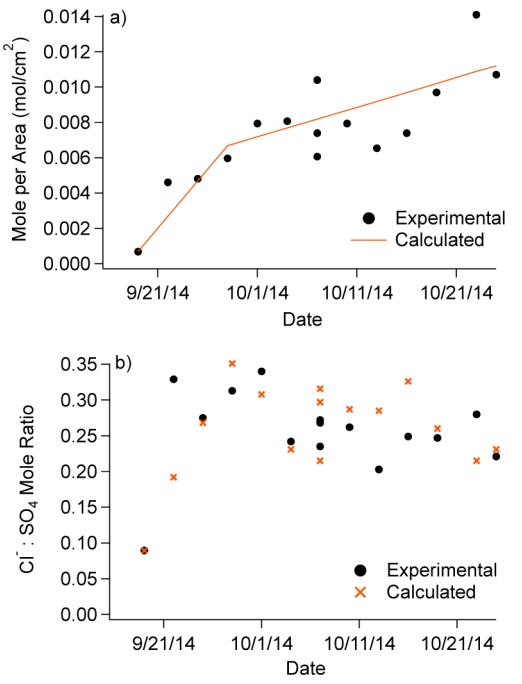

Figure 3. Comparison of experimental (black) and calculated (orange) values for a) moles of chloride per area and b) sulfate normalized moles of chloride in grime over time.

concentration in the film maintained for over a month. However, this does not exclude the possibility of an additional source from HCl or a chloride source from the deposition of particles greater than 10 μm in diameter. The scatter in the sodium data limits the certainty of carrying out a similar analysis for this ion.

The calcium-to-sulfate mole ratios in the grime also show a gradual increase over time (Figure 2d). In this case, the calcium-to-sulfate ratio for the final two particle samples are also higher than the first 3 samples, and thus the film may be responding to these changes. Chabas et al. suggested the possibility of the leaching of calcium from the glass into the film both through the reactions with gas phase species as mentioned above or through cation exchange with film protons.[22,56] One would also expect an enhancement of these ions if there were a large input of particles larger than PM_{10}. However, because there does not seem to be a large difference between the calcium-to-sulfate ratios between the film and particles these processes do not seem to be playing a large role under the present conditions. The times of greatest discrepancy can be attributed to the film's slow response to decreasing particle concentrations, as discussed for chloride.

Photochemical Processing of Nitrate. Previous work from our lab[41,42] and others[57] has shown that nitrate deposited onto environmental surfaces as HNO_3 shows rapid photochemical loss, orders of magnitude faster than aqueous nitrate, and that this process is a potential renoxification mechanism in the environment. As part of the present campaign, we explored such a loss process from ambient film samples. This was probed by collecting samples both exposed to and shielded from sunlight. Figure 4 displays the ratio of the light-to-dark mole fractions of the ions investigated here over the course of the campaign. One expects that the ions that are neither photolabile nor photoproducts will show no preference for light versus dark, therefore showing a ratio of unity for the

DOI: 10.1021/acs.est.5b03054
Environ. Sci. Technol. XXXX, XXX, XXX−XXX

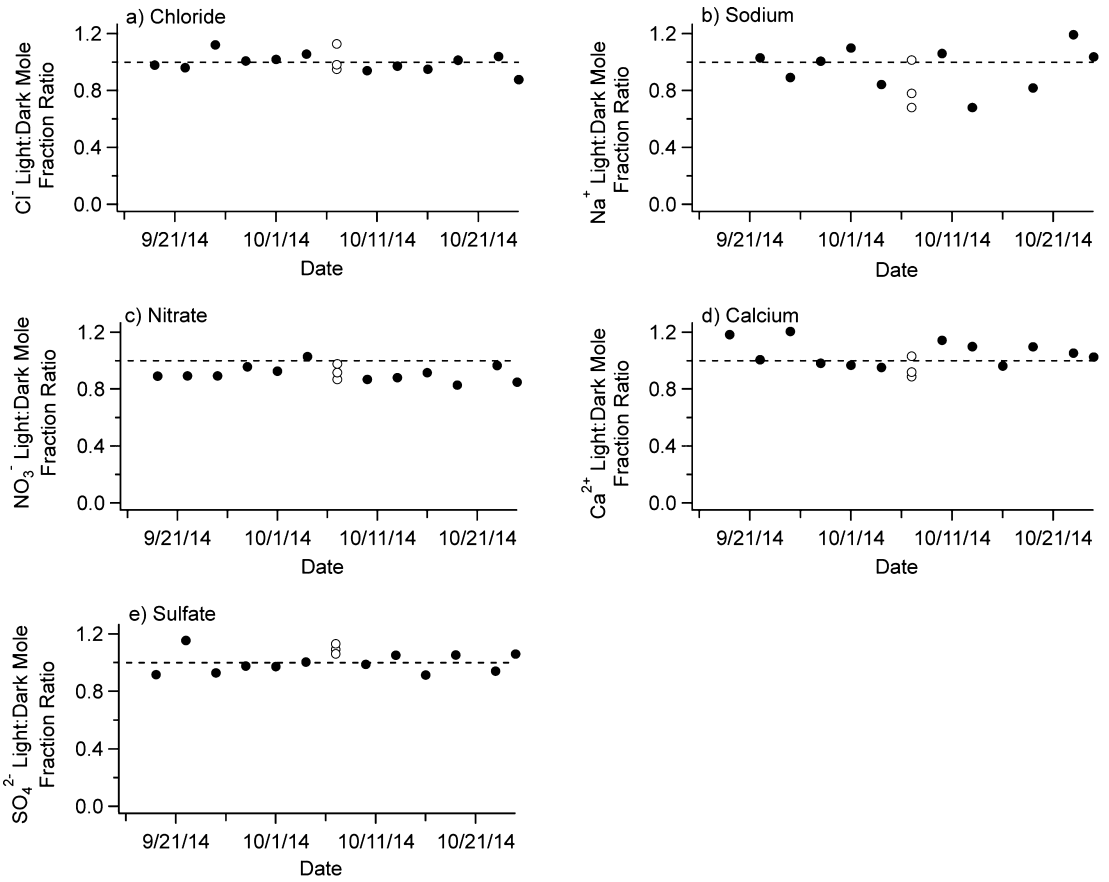

Figure 4. Light-to-dark ratio for the mole fractions of ions extracted from the film. In each case, the dotted line shows a ratio of unity. a) Chloride, showing a light:dark ratio of 1.00 ± 0.06. b) Sodium: 0.99 ± 0.2. c) Nitrate: 0.90 ± 0.05. d) Calcium: 1.03 ± 0.09. e) Sulfate: 1.03 ± 0.06. Values given for the light:dark ratio are the campaign average ±1 standard deviation.

duration of the experiment. This is indeed seen for the majority of the ions within the film, with the ratios scattered around a value of 1.0.

The notable exception is nitrate, whose average light-to-dark ratio is 0.90 ± 0.05, which is statistically lower than unity with greater than 99% confidence. The 10% difference between the light-exposed and nonexposed samples, maintained over the entire campaign, is consistent with a photochemical loss pathway for film-associated nitrate observed in the laboratory studies.[41,42,57] We note that a slight temperature gradient between the dark and light samples cannot be ruled out, raising the possibility of enhanced nitrate loss by ammonium nitrate evaporation from the light-exposed sample.[48,49] However, we do not observe any greater amounts of ammonium ion in the dark film sample than in the light-exposed one, suggesting that this pathway is probably not important here.

DISCUSSION

Diamond and co-workers have demonstrated that urban grime films can increase the mobility of species in the environment, both by being a temporary reservoir for organic species to partition into and through film wash-off during precipitation events.[10,11,31,32] In the present study we see not only this increased mobility in the volatilization of ammonium nitrate but also evidence for potential chemical transformations of inorganic ions. As shown in Figure 2, the grime film's composition changes over time in a way distinct from that seen in the surrounding particles, despite the particles being a major source of ions to the film. Following deposition onto a hygroscopic urban surface, particles of different composition and size are subject to mixing when water is taken up onto the grime film. In this medium, further processing is possible through reaction or through the exchange of gas phase species, which can be released from or deposited onto the surface.

One such species is ammonia, a basic gas that plays an important role in particle nucleation and neutralizing aerosols, reacting with acidic species to form ammonium.[46] While ammonium is clearly present in the particles we monitored here, we do not measure quantifiable amounts of ammonium in grime, suggesting a loss of ammonium during the grime film formation and growth. There are different hypotheses to explain this loss, but it is clear that deposition to the film is altering the cycling of ammonium in the environment, in contrast to a simple deposition framework. It has been shown that it is important to use a scheme including bidirectional ammonia flux when describing atmosphere-biosphere interactions.[58] Our results demonstrate that bidirectional exchange between urban grime films and the surrounding atmosphere may also need to be considered to understand urban atmospheric chemistry. A study of the grime pH could give insight into the ammonia-ammonium equilibrium on the film and the corresponding ammonia vapor pressure, in order to obtain the potential for ammonia release. However, during this campaign, the observed low level of grime ammonium suggests that the film was releasing ammonia back into the atmosphere. A study completed in Toronto observed a significant ammonia source within a street canyon, attributing this to the green space

DOI: 10.1021/acs.est.5b03054
Environ. Sci. Technol. XXXX, XXX, XXX−XXX

contained within the canyon;[59] however, if ammonium is being lost from grime, then the urban films formed along the building could also be playing a role in the ammonia gradient measured.

A further impact of the film environment on the nitrogen cycling is nitrate photolysis in the grime. Over the campaign, nitrate samples exposed to solar illumination showed statistically significant lower nitrate concentrations than the corresponding dark samples, providing the first direct field evidence for nitrate photochemistry in urban grime. Studies are still ongoing to classify the gas phase products of the nitrate chemistry in grime; however, earlier studies of nitrate photolysis in water and on ice, metal oxides, and glass suggest that this photochemistry would lead to the formation of the reactive nitrogen species NO, NO_2, and HONO (e.g. refs 42, 57, 60, and 61). Thus, the observed photolability of film nitrate could provide a renoxification process in the urban environment. We note that such processes could contribute to unknown reactive nitrogen sources such as a fixed photochemical source of HONO within 20 m of the ground found in Houston, TX.[62,63]

Another aspect of the grime-associated atmospheric processing is "capture events", in which particular ions are elevated due to an influx of these species associated with a particular population of particles. As seen here, particulate chloride can be episodic in nature such as when marine-influenced particles are transported inland or in regions where chloride salts are used for snow management. When particulate chloride levels are high, large amounts of chloride can be captured on the film extending the period in which elevated chloride levels are exposed to the atmosphere. Chloride levels are of interest due to known heterogeneous reaction between N_2O_5 and chloride to form $ClNO_2$.[5] This reaction, which also produces nitrate anion, releases active chlorine and nitrogen in the morning when $ClNO_2$ photolyzes thereby increasing the oxidative capacity of the atmosphere.[4,64] Although previously thought of as only important in marine regions, there have now been multiple observations of $ClNO_2$ in midcontinental environments through reaction of N_2O_5 with chloride attributed to transported sea spray, biomass burning, and coal fired power plants.[65,66] $ClNO_2$ production is limited by the availability of chloride which is currently defined in terms of the sum of particulate chloride and HCl.[66,67] However, the chloride captured on the film may also be available for reaction with N_2O_5, which in turn could impact the $ClNO_2$ production in these urban continental regions.

In summary, by comparing the composition of particles and urban grime films collected simultaneously, several possible processes were elucidated that add to our understanding of grime film formation; as well, these processes suggest that urban grime films could have an important environmental impact. These possibilities include the potential for grime to act as a source of $ClNO_2$ as well as to recycle ammonia and reactive nitrogen back into the atmosphere. Further study into these processes is warranted.

■ ASSOCIATED CONTENT

Supporting Information

The Supporting Information is available free of charge on the ACS Publications website at DOI: 10.1021/acs.est.5b03054.

Information on sampling site, meteorological conditions, and gas phase species present during the measurement period, absolute particle and grime concentrations, and size resolved particle composition for the final 5 days of measurement (PDF)

■ AUTHOR INFORMATION

Corresponding Author

*Phone: 1/416 978 3603. E-mail: jdonalds@chem.utoronto.ca.

Present Address

[§]Department of Chemistry, University of Alberta, 11227 Saskatchewan Drive, Edmonton, AB, Canada T6G 2G2.

Notes

The authors declare no competing financial interest.

■ ACKNOWLEDGMENTS

The authors acknowledge the technical support of O. Böge, A. Dietze, S. Fuchs, R. Gräfe, A. Grüner, C. Kurze, A. Rödger, and G. Spindler. We appreciate the support of the Saxon State Agency for Environment, Agriculture and Geology (LfULG) in conducting the sampling at Leipzig-Mitte as well as their provision of additional data. We thank NSERC for ongoing financial support. A.M.B. acknowledges NSERC for the award of a CGS-D graduate fellowship and the Chemistry Department of the University of Toronto for travel support.

■ REFERENCES

(1) Ravishankara, A. R. Heterogeneous and Multiphase Chemistry in the Troposphere. *Science* **1997**, *276*, 1058−1065.

(2) Chang, W. L.; Bhave, P. V.; Brown, S. S.; Riemer, N.; Stutz, J.; Dabdub, D. Heterogeneous Atmospheric Chemistry, Ambient Measurements, and Model Calculations of N_2O_5: A Review. *Aerosol Sci. Technol.* **2011**, *45*, 665−695.

(3) Finlayson-Pitts, B. J.; Wingen, L. M.; Sumner, A. L.; Syomin, D.; Ramazan, K. A. The Heterogeneous Hydrolysis of NO_2 In Laboratory Systems and in Outdoor and Indoor Atmospheres: an Integrated Mechanism. *Phys. Chem. Chem. Phys.* **2003**, *5*, 223−242.

(4) Riedel, T. P.; Wolfe, G. M.; Danas, K. T.; Gilman, J. B.; Kuster, W. C.; Bon, D. M.; Vlasenko, A.; Li, S. M.; Williams, E. J.; Lerner, B. M.; et al. An MCM Modeling Study of Nitryl Chloride ($ClNO_2$) Impacts on Oxidation, Ozone Production and Nitrogen Oxide Partitioning in Polluted Continental Outflow. *Atmos. Chem. Phys.* **2014**, *14*, 3789−3800.

(5) Finlayson-Pitts, B. J.; Ezell, M. J.; Pitts, J. N. Formation of Chemically Active Chlorine Compounds by Reactions of Atmospheric NaCl Particles with Gaseous N_2O_5 And $ClONO_2$. *Nature* **1989**, *337*, 241−244.

(6) Harris, E.; Sinha, B.; Foley, S.; Crowley, J. N.; Borrmann, S.; Hoppe, P. Sulfur Isotope Fractionation During Heterogeneous Oxidation of SO_2 On Mineral Dust. *Atmos. Chem. Phys.* **2012**, *12*, 4867−4884.

(7) Usher, C. R.; Michel, A. E.; Grassian, V. H. Reactions on Mineral Dust. *Chem. Rev.* **2003**, *103*, 4883−4939.

(8) Mamane, Y.; Gottlieb, J. Heterogeneous Reactions of Minerals with Sulfur and Nitrogen Oxides. *J. Aerosol Sci.* **1989**, *20*, 303−311.

(9) George, C.; Ammann, M.; D'Anna, B.; Donaldson, D. J.; Nizkorodov, S. A. Heterogeneous Photochemistry in the Atmosphere. *Chem. Rev.* **2015**, *115*, 4218−4258.

(10) Diamond, M. L.; Priemer, D. A.; Law, N. L. Developing a Multimedia Model of Chemical Dynamics in an Urban Area. *Chemosphere* **2001**, *44*, 1655−1667.

(11) Csiszar, S. A.; Diamond, M. L.; Thibodeaux, L. J. Modeling Urban Films Using a Dynamic Multimedia Fugacity Model. *Chemosphere* **2012**, *87*, 1024−1031.

(12) Diamond, M. L.; Gingrich, S. E.; Fertuck, K.; McCarry, B. E.; Stern, G. A.; Billeck, B.; Grift, B.; Brooker, D.; Yager, T. D. Evidence for Organic Film on an Impervious Urban Surface: Characterization and Potential Teratogenic Effects. *Environ. Sci. Technol.* **2000**, *34*, 2900−2908.

DOI: 10.1021/acs.est.5b03054
Environ. Sci. Technol. XXXX, XXX, XXX−XXX

(13) Law, N. L.; Diamond, M. L. The Role of Organic Films and the Effect on Hydrophobic Organic Compounds in Urban Areas: an Hypothesis. *Chemosphere* **1998**, *36*, 2607−2620.
(14) Simpson, A. J.; Lam, B.; Diamond, M. L.; Donaldson, D. J.; Lefebvre, B. A.; Moser, A. Q.; Williams, A. J.; Larin, N. I.; Kvasha, M. P. Assessing the Organic Composition of Urban Surface Films Using Nuclear Magnetic Resonance Spectroscopy. *Chemosphere* **2006**, *63*, 142−152.
(15) Liu, Q.-T.; Chen, R.; McCarry, B. E.; Diamond, M. L.; Bahavar, B. Characterization of Polar Organic Compounds in the Organic Film on Indoor and Outdoor Glass Windows. *Environ. Sci. Technol.* **2003**, *37*, 2340−2349.
(16) Lam, B.; Diamond, M. L.; Simpson, A. J.; Makar, P. A.; Truong, J.; Hernandez-Martinez, N. A. Chemical Composition of Surface Films on Glass Windows and Implications for Atmospheric Chemistry. *Atmos. Environ.* **2005**, *39*, 6578−6586.
(17) Lombardo, T.; Ionescu, A.; Lefèvre, R. A.; Chabas, A.; Ausset, P.; Cachier, H. Soiling of Silica-Soda-Lime Float Glass in Urban Environment: Measurements and Modelling. *Atmos. Environ.* **2005**, *39*, 989−997.
(18) Favez, O.; Cachier, H.; Chabas, A.; Ausset, P.; Lefevre, R. Crossed Optical and Chemical Evaluations of Modern Glass Soiling in Various European Urban Environments. *Atmos. Environ.* **2006**, *40*, 7192−7204.
(19) Lombardo, T.; Ionescu, A.; Chabas, A.; Lefevre, R.; Ausset, P.; Candau, Y. Dose−Response Function for the Soiling of Silica−Soda−Lime Glass Due to Dry Deposition. *Sci. Total Environ.* **2010**, *408*, 976−984.
(20) Ionescu, A.; Lefèvre, R. A.; Chabas, A.; Lombardo, T.; Ausset, P.; Candau, Y.; Rosseman, L. Modeling of Soiling Based on Silica-Soda-Lime Glass Exposure at Six European Sites. *Sci. Total Environ.* **2006**, *369*, 246−255.
(21) Alfaro, S.; Chabas, A.; Lombardo, T.; Verney-Carron, A.; Ausset, P. Predicting the Soiling of Modern Glass in Urban Environments: a New Physically-Based Model. *Atmos. Environ.* **2012**, *60*, 348−357.
(22) Chabas, A.; Lombardo, T.; Cachier, H.; Pertuisot, M. H.; Oikonomou, K.; Falcone, R.; Verità, M.; Geotti-Bianchini, F. Behaviour of Self-Cleaning Glass in Urban Atmosphere. *Build Environ* **2008**, *43*, 2124−2131.
(23) Duigu, J. R.; Ayoko, G. A.; Kokot, S. Building and Environment. *Build Environ* **2009**, *44*, 2228−2235.
(24) Wu, R. W.; Harner, T.; Diamond, M. L. Evolution Rates and PCB Content of Surface Films That Develop on Impervious Urban Surfaces. *Atmos. Environ.* **2008**, *42*, 6131−6143.
(25) Wu, R. W.; Harner, T.; Diamond, M. L.; Wilford, B. Partitioning Characteristics of PCBs in Urban Surface Films. *Atmos. Environ.* **2008**, *42*, 5696−5705.
(26) Chabas, A.; Alfaro, S.; Lombardo, T.; Verney-Carron, A.; Da Silva, E.; Triquet, S.; Cachier, H.; Leroy, E. Long Term Exposure of Self-Cleaning and Reference Glass in an Urban Environment: a Comparative Assessment. *Build Environ* **2014**, *79*, 57−65.
(27) Lombardo, T.; Chabas, A.; Verney-Carron, A.; Cachier, H.; Triquet, S.; Darchy, S. Physico-Chemical Characterization of Glass Soiling in Rural, Urban and Industrial Environments. *Environ. Sci. Pollut. Res.* **2014**, *21*, 9251−9258.
(28) Alfaro, S. C.; Chabas, A.; Lombardo, T.; Verney-Carron, A.; Ausset, P. Predicting the Soiling of Modern Glass in Urban Environments: a New Physically-Based Model. *Atmos. Environ.* **2012**, *60*, 348−357.
(29) Verney-Carron, A.; Dutot, A. L.; Lombardo, T.; Chabas, A. Predicting Changes of Glass Optical Properties in Polluted Atmospheric Environment by a Neural Network Model. *Atmos. Environ.* **2012**, *54*, 141−148.
(30) Lombardo, T.; Ionescu, A.; Chabas, A.; Lefèvre, R. A.; Ausset, P.; Candau, Y. Dose−Response Function for the Soiling of Silica−Soda−Lime Glass Due to Dry Deposition. *Sci. Total Environ.* **2010**, *408*, 976−984.
(31) Priemer, D. A.; Diamond, M. L. Application of the Multimedia Urban Model to Compare the Fate of SOCs in an Urban and Forested Watershed. *Environ. Sci. Technol.* **2002**, *36*, 1004−1013.
(32) Diamond, M. L.; Melymuk, L.; Csiszar, S. A.; Robson, M. Estimation of PCB Stocks, Emissions, and Urban Fate: Will Our Policies Reduce Concentrations and Exposure? *Environ. Sci. Technol.* **2010**, *44*, 2777−2783.
(33) Monge, M. E.; D'Anna, B.; Mazri, L.; Giroir-Fendler, A.; Ammann, M.; Donaldson, D. J.; George, C. Light Changes the Atmospheric Reactivity of Soot. *Proc. Natl. Acad. Sci. U. S. A.* **2010**, *107*, 6605−6609.
(34) Brigante, M.; Cazoir, D.; D'Anna, B.; George, C.; Donaldson, D. J. Photoenhanced Uptake of NO_2 By Pyrene Solid Films. *J. Phys. Chem. A* **2008**, *112*, 9503−9508.
(35) Cazoir, D.; Brigante, M.; Ammar, R.; D'Anna, B.; George, C. Heterogeneous Photochemistry of Gaseous NO_2 On Solid Fluoranthene Films: a Source of Gaseous Nitrous Acid (HONO) in the Urban Environment. *J. Photochem. Photobiol., A* **2014**, *273*, 23−28.
(36) Styler, S. A.; Brigante, M.; D'Anna, B.; George, C.; Donaldson, D. J. Photoenhanced Ozone Loss on Solid Pyrene Films. *Phys. Chem. Chem. Phys.* **2009**, *11*, 7876−7884.
(37) George, C.; Strekowski, R. S.; Kleffmann, J.; Stemmler, K.; Ammann, M. Photoenhanced Uptake of Gaseous NO2 on Solid-Organic Compounds: a Photochemical Source of HONO? *Faraday Discuss.* **2005**, *130*, 195−210.
(38) Kahan, T. F.; Kwamena, N. O. A.; Donaldson, D. J. Heterogeneous Ozonation Kinetics of Polycyclic Aromatic Hydrocarbons on Organic Films. *Atmos. Environ.* **2006**, *40*, 3448−3459.
(39) Kwamena, N.-O. A.; Clarke, J. P.; Kahan, T. F.; Diamond, M. L.; Donaldson, D. J. Assessing the Importance of Heterogeneous Reactions of Polycyclic Aromatic Hydrocarbons in the Urban Atmosphere Using the Multimedia Urban Model. *Atmos. Environ.* **2007**, *41*, 37−50.
(40) Ammar, R.; Monge, M. E.; George, C.; D'Anna, B. Photoenhanced NO_2 Loss on Simulated Urban Grime. *ChemPhysChem* **2010**, *11*, 3956−3961.
(41) Handley, S. R.; Clifford, D.; Donaldson, D. J. Photochemical Loss of Nitric Acid on Organic Films: a Possible Recycling Mechanism for NO_X. *Environ. Sci. Technol.* **2007**, *41*, 3898−3903.
(42) Baergen, A. M.; Donaldson, D. J. Photochemical Renoxification of Nitric Acid on Real Urban Grime. *Environ. Sci. Technol.* **2013**, *47*, 815−820.
(43) Engler, C.; Birmili, W.; Spindler, G.; Wiedensohler, A. Analysis of Exceedances in the Daily PM_{10} Mass Concentration (50 Mgm^{-3}) At a Roadside Station in Leipzig, Germany. *Atmos. Chem. Phys.* **2012**, *12*, 10107−10123.
(44) Creighton, P. J.; Lioy, P. J.; Haynie, F. H.; Lemmons, T. J.; Miller, J. L.; Gerhart, J. Soiling by Atmospheric Aerosols in an Urban Industrial Area. *J. Air Waste Manage. Assoc.* **1990**, *40*, 1285−1289.
(45) Berner, A.; Luerzer, C. Mass Size Distributions of Traffic Aerosols at Vienna. *J. Phys. Chem.* **1980**, *84*, 2079.
(46) Finlayson-Pitts, B. J.; Pitts, J. N., Jr. *Chemistry of the Upper and Lower Atmosphere: Theory, Experiments, and Applications*; Academic Press: San Diego, CA, 1999.
(47) Herrmann, H.; Brüggemann, E.; Franck, U.; Gnauk, T.; Löschau, G.; Müller, K.; Plewka, A.; Spindler, G. A Source Study of PM in Saxony by Size-Segregated Characterisation. *J. Atmos. Chem.* **2006**, *55*, 103−130.
(48) Du, H.; Kong, L.; Cheng, T.; Chen, J.; Yang, X.; Zhang, R.; Han, Z.; Yan, Z.; Ma, Y. Insights Into Ammonium Particle-to-Gas Conversion: Non-Sulfate Ammonium Coupling with Nitrate and Chloride. *Aerosol Air Qual. Res.* **2010**, *10*, 589−595.
(49) Schaap, M.; Spindler, G.; Schulz, M.; Acker, K.; Maenhaut, W.; Berner, A.; Wieprecht, W.; Streit, N.; Müller, K.; Brüggemann, E.; et al. Artefacts in the Sampling of Nitrate Studied in the "INTERCOMP" Campaigns of EUROTRAC-AEROSOL. *Atmos. Environ.* **2004**, *38*, 6487−6496.

DOI: 10.1021/acs.est.5b03054
Environ. Sci. Technol. XXXX, XXX, XXX−XXX

(50) Hodzic, A.; Bessagnet, B.; Vautard, R. A Model Evaluation of Coarse-Mode Nitrate Heterogeneous Formation on Dust Particles. *Atmos. Environ.* **2006**, *40*, 4158−4171.
(51) VandenBoer, T. C.; Petroff, A.; Markovic, M. Z.; Murphy, J. G. Size Distribution of Alkyl Amines in Continental Particulate Matter and Their Online Detection in the Gas and Particle Phase. *Atmos. Chem. Phys.* **2011**, *11*, 4319−4332.
(52) Pathak, R. K.; Chan, C. K. Inter-Particle and Gas-Particle Interactions in Sampling Artifacts of $PM_{2.5}$ In Filter-Based Samplers. *Atmos. Environ.* **2005**, *39*, 1597.
(53) Hennigan, C. J.; Izumi, J.; Sullivan, A. P.; Weber, R. J.; Nenes, A. A Critical Evaluation of Proxy Methods Used to Estimate the Acidity of Atmospheric Particles. *Atmos. Chem. Phys.* **2015**, *15*, 2775−2790.
(54) Draxler, R. R.; Rolph, G. D. *HYPSPLIT (HYbrid Single-Particle Lagrangian Integrated Trajectory) Model Access via NOAA ARL READY Website*; NOAA Air Resources Laboratory: College Park, MD. Http://Www.Arl.Noaa.Gov/HYSPLIT.Php (accessed Oct 1, 2015).
(55) Möller, D.; Acker, K. Chlorine-Phase Partitioning at Melpitz Near Leipzig. In *Nucleation and Atmospheric Aerosols*; 17th International Conference, Galway, Ireland, 2007, Springer Netherlands: 2007; pp 654−658.
(56) Lombardo, T.; Chabas, A.; Lefèvre, R. A.; Verità, M.; Geotti-Bianchini, F. Weathering of Float Glass Exposed Outdoors in an Urban Area. *Glass Technol.* **2005**, *46*, 271−276.
(57) Zhou, X.; Gao, H.; He, Y.; Huang, G.; Bertman, S. B.; Civerolo, K.; Schwab, J. Nitric Acid Photolysis on Surfaces in Low-NO_X Environments: Significant Atmospheric Implications. *Geophys. Res. Lett.* **2003**, *30*, 2217.
(58) Flechard, C. R.; Massad, R. S.; Loubet, B.; Personne, E.; Simpson, D.; Bash, J. O.; Cooter, E. J.; Nemitz, E.; Sutton, M. A. Advances in Understanding, Models and Parameterizations of Biosphere-Atmosphere Ammonia Exchange. *Biogeosciences* **2013**, *10*, 5183−5225.
(59) Hu, Q.; Zhang, L.; Evans, G. J.; Yao, X. Variability of Atmospheric Ammonia Related to Potential Emission Sources in Downtown Toronto, Canada. *Atmos. Environ.* **2014**, *99*, 365−373.
(60) Grannas, A. M.; Jones, A. E.; Dibb, J.; Ammann, M.; Anastasio, C.; Beine, H. J.; Bergin, M.; Bottenheim, J.; Boxe, C. S.; Carver, G.; et al. An Overview of Snow Photochemistry: Evidence, Mechanisms and Impacts. *Atmos. Chem. Phys.* **2007**, *7*, 4329−4373.
(61) Nanayakkara, C. E.; Jayaweera, P. M.; Rubasinghege, G.; Baltrusaitis, J.; Grassian, V. H. Surface Photochemistry of Adsorbed Nitrate: the Role of Adsorbed Water in the Formation of Reduced Nitrogen Species on α-Fe_2O_3 Particle Surfaces. *J. Phys. Chem. A* **2014**, *118*, 158−166.
(62) Wong, K. W.; Tsai, C.; Lefer, B.; Grossberg, N.; Stutz, J. Modeling of Daytime HONO Vertical Gradients During SHARP 2009. *Atmos. Chem. Phys.* **2013**, *13*, 3587−3601.
(63) Wong, K. W.; Tsai, C.; Lefer, B.; Haman, C.; Grossberg, N.; Brune, W. H.; Ren, X.; Luke, W.; Stutz, J. Daytime HONO Vertical Gradients During SHARP 2009 in Houston, TX. *Atmos. Chem. Phys.* **2012**, *12*, 635−652.
(64) Simpson, W. R.; Brown, S. S.; Saiz-Lopez, A.; Thornton, J. A.; Glasow, R. V. Tropospheric Halogen Chemistry: Sources, Cycling, and Impacts. *Chem. Rev.* **2015**, *115*, 4035−4062.
(65) Mielke, L. H.; Furgeson, A.; Osthoff, H. D. Observation of $ClNO_2$ In a Mid-Continental Urban Environment. *Environ. Sci. Technol.* **2011**, *45*, 8889−8896.
(66) Thornton, J. A.; Kercher, J. P.; Riedel, T. P.; Wagner, N. L.; Cozic, J.; Holloway, J. S.; Dubé, W. P.; Wolfe, G. M.; Quinn, P. K.; Middlebrook, A. M.; et al. A Large Atomic Chlorine Source Inferred From Mid-Continental Reactive Nitrogen Chemistry. *Nature* **2010**, *464*, 271−274.
(67) Simon, H.; Kimura, Y.; McGaughey, G.; Allen, D. T.; Brown, S. S.; Coffman, D.; Dibb, J.; Osthoff, H. D.; Quinn, P.; Roberts, J. M. Modeling Heterogeneous $ClNO_2$ Formation, Chloride Availability, and Chlorine Cycling in Southeast Texas. *Atmos. Environ.* **2010**, *44*, 5476−5488.

DOI: 10.1021/acs.est.5b03054
Environ. Sci. Technol. XXXX, XXX, XXX−XXX